AEDC-TR-79-40

cy 2

A CORRELATION OF ARTIFICALLY INDUCED BOUNDARY-LAYER TRANSITION DATA FROM BLUNT SLENDER CONES AT HYPERSONIC SPEEDS

A. H. Boudreau
ARO, Inc., a Sverdrup Corporation Company

VON KÁRMÁN GAS DYNAMICS FACILITY
ARNOLD ENGINEERING DEVELOPMENT CENTER
AIR FORCE SYSTEMS COMMAND
ARNOLD AIR FORCE STATION, TENNESSEE 37389

June 1979

Final Report for Period July 13, 1978 — August 16, 1978

Prepared for

ARNOLD ENGINEERING DEVELOPMENT CENTER/DOTR
ARNOLD AIR FORCE STATION, TENNESSEE 37389

NOTICES

When U. S. Government drawings, specifications, or other data are used for any purpose other than a definitely related Government procurement operation, the Government thereby incurs no responsibility nor any obligation whatsoever, and the fact that the Government may have formulated, furnished, or in any way supplied the said drawings, specifications, or other data, is not to be regarded by implication or otherwise, or in any manner licensing the holder or any other person or corporation, or conveying any rights or permission to manufacture, use, or sell any patented invention that may in any way be related thereto.

Qualified users may obtain copies of this report from the Defense Documentation Center.

References to named commerical products in this report are not to be considered in any sense as an indorsement of the product by the United States Air Force or the Government.

This report has been reviewed by the Information Office (OI) and is releasable to the National Technical Information Service (NTIS). At NTIS, it will be available to the general public, including foreign nations.

APPROVAL STATEMENT

This report has been reviewed and approved.

Elton R. Thompson

ELTON R. THOMPSON
Project Manager, Research Division
Directorate of Test Engineering

Approved for publication:

FOR THE COMMANDER

Robert W. Crossley

ROBERT W. CROSSLEY, Lt Colonel, USAF
Acting Director of Test Engineering
Deputy for Operations

REPORT DOCUMENTATION PAGE

READ INSTRUCTIONS BEFORE COMPLETING FORM

1. REPORT NUMBER: AEDC-TR-79-40	2. GOVT ACCESSION NO.
3. RECIPIENT'S CATALOG NUMBER	
4. TITLE (and Subtitle): A CORRELATION OF ARTIFICIALLY INDUCED BOUNDARY-LAYER TRANSITION DATA FROM BLUNT SLENDER CONES AT HYPERSONIC SPEEDS	5. TYPE OF REPORT & PERIOD COVERED: Final Report - July 13, 1978 - August 16, 1978
	6. PERFORMING ORG. REPORT NUMBER
7. AUTHOR(s): A. H. Boudreau, ARO, Inc., a Sverdrup Corporation Company	8. CONTRACT OR GRANT NUMBER(s)
9. PERFORMING ORGANIZATION NAME AND ADDRESS: Arnold Engineering Development Center/DOTR, Air Force Systems Command, Arnold Air Force Station, Tennessee 37389	10. PROGRAM ELEMENT, PROJECT, TASK AREA & WORK UNIT NUMBERS: Program Element 65807F
11. CONTROLLING OFFICE NAME AND ADDRESS: Arnold Engineering Development Center/OIS, Air Force Systems Command, Arnold Air Force Station, Tennessee 37389	12. REPORT DATE: June 1979
	13. NUMBER OF PAGES: 7
14. MONITORING AGENCY NAME & ADDRESS (if different from Controlling Office)	15. SECURITY CLASS. (of this report): UNCLASSIFIED
	15a. DECLASSIFICATION/DOWNGRADING SCHEDULE: N/A

16. DISTRIBUTION STATEMENT (of this Report)

Approved for public release; distribution unlimited.

17. DISTRIBUTION STATEMENT (of the abstract entered in Block 20, if different from Report)

18. SUPPLEMENTARY NOTES

Available in DDC

19. KEY WORDS (Continue on reverse side if necessary and identify by block number)

boundary layer transition
blunt bodies
nose cones
hypersonic flow
wind tunnels
surface roughness
data bases

20. ABSTRACT (Continue on reverse side if necessary and identify by block number)

Previous investigations of distributed-roughness boundary-layer trips indicated that they are superior to spherical-type trips in that equally effective distributed-roughness trips are one-fifth as high and produce substantially smaller flow-field disturbances. The present work has expanded the data base, permitting correlation of distributed roughness tripping data. The correlation thus developed includes a wide range of Reynolds numbers, cone angles, and trip heights. Plots are provided that permit the selection of distributed-roughness trips without the need of boundary-layer solutions.

DD FORM 1 JAN 73 1473 EDITION OF 1 NOV 65 IS OBSOLETE

PREFACE

The work described herein was conducted by the Arnold Engineering Development Center (AEDC), Air Force Systems Command (AFSC), Arnold Air Force Station, Tennessee. The research results were obtained by personnel of ARO, Inc., AEDC Division, contract operator of the AEDC. The work was done under ARO Project V32A-P6A, and the manuscript was submitted for publication on April 27, 1979.

Abstract

Previous investigations of distributed-roughness boundary-layer trips indicated that they are superior to spherical-type trips in that equally effective distributed-roughness trips are one-fifth as high and produce substantially smaller flow-field disturbances. The present work has expanded the data base, permitting correlation of distributed roughness tripping data. The correlation thus developed includes a wide range of Reynolds numbers, cone angles, and trip heights. Plots are provided that permit the selection of distributed-roughness trips without the need of boundary-layer solutions.

Nomenclature

k	Trip element height, in.
M_∞	Free-stream Mach number
P_E	Pressure at the end of the roughness area ($s/r_n = 5$), psia
P'_o	Free-stream pitot pressure, psia
p_∞	Free-stream pressure, psia
q_∞	Free-stream dynamic pressure, psia
$Re_{e,\theta}$	Reynolds number based on boundary-layer edge conditions and momentum thickness
Re_{e,r_n}	Reynolds number based on boundary-layer edge conditions and model nose radius
Re_∞/ft	Reynolds number based on free-stream conditions and a 1-ft length
Re_{∞,r_n}	Reynolds number based on free-stream conditions and model nose radius
r_b	Model base radius, in.
r_n	Model nose radius, in.
s	Surface distance along the model measured from the stagnation point, in.
T_e	Temperature at the edge of the boundary layer, $^\circ R$
T_{o_∞}	Free-stream total temperature, $^\circ R$
T_w	Model wall temperature, $^\circ R$
T_∞	Free-stream temperature, $^\circ R$
X	Mayne's correlation parameter [see Eq. (3)]
θ	Boundary-layer momentum thickness, in.
θ_c	Model cone half-angle, deg
λ	PANT correlation parameter [see Eq. (1)]
λ^*_M	Modified PANT correlation parameter evaluated at the sonic point [see Eq. (5)]

Subscripts

critical	The value of the parameter needed to bring transition up to or near the trip
t	At the end of transition

Superscripts

*	Evaluated at the sonic point

1.0 Introduction

Previous work[1] in the AEDC-VKF on distributed-roughness boundary-layer trips identified the optimum types and placement of trips. These tests indicated the clear advantage of using distributed-roughness-type trips instead of the commonly employed spherical trips since distributed-roughness trips were one-fifth as large as spherical trips yet provided the same trip effectiveness, thus implying significantly less flow-field disturbance. The previous tests were limited, however, to a 7-deg blunt cone tested over a very limited Reynolds number range. Thus, the data base was insufficient to develop a meaningful correlation.

The present work has been directed toward expanding the data base and developing a prediction technique. A primary objective in developing this correlation was to make its use independent of further boundary-layer solutions. Hence, plots have been developed (Appendix A of this paper) that allow the reader to size trips using only the information in this paper.

2.0 Experimental Apparatus

2.1 AEDC-VKF Tunnel F

Tunnel F is an arc-driven wind tunnel of the hotshot type,[2,3] and capable of providing Mach numbers from about 7 to 13 over a Reynolds number per foot range from 0.20×10^6 to 50×10^6.

This test was conducted using the 40-in.-exit-diam contoured nozzle in the 54-in.-diam test section to obtain a nominal free-stream Mach number of 9.0. Nitrogen was the test gas. Because of the relatively short (100-msec) test times, the model wall temperature remained essentially invariant from the initial value of approximately 540°R; thus $T_w/T_{o_\infty} \cong 0.15$ to 0.35, which approximates the condition of practical interest for reentry vehicles.

2.2 Models

Models for the latest entry consisted of an r_n = 0.5-in., 5-deg, half-angle cone and an

r_n = 0.589-in., 7-deg, half-angle cone with an alternate 14-deg biconic nose section. These models are shown in Figs. 1, 2, and 3, respectively. The primary instrumentation on these models was coaxial heat-transfer gages. The trips used in this entry were identical to those used in the previous tests[1] and are described in Table 1.

2.3 Instrumentation

Coaxial surface thermocouple gages were used to measure the surface heating-rate distributions. In practical measurement applications, the surface thermocouple behaves as a homogeneous, one-dimensional, semi-infinite solid. The instrument provides an electromotive force (EMF) directly proportional to surface temperature that may be related by theory to the incident heat flux. All heat-transfer gages were bench calibrated before installation into the model. The precision of these calibrations is estimated to be ±3 percent. The gages were supplied and installed by AEDC-VKF.

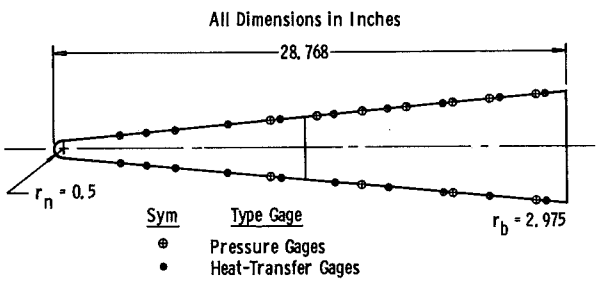

Fig. 1. The 5-deg Cone Model

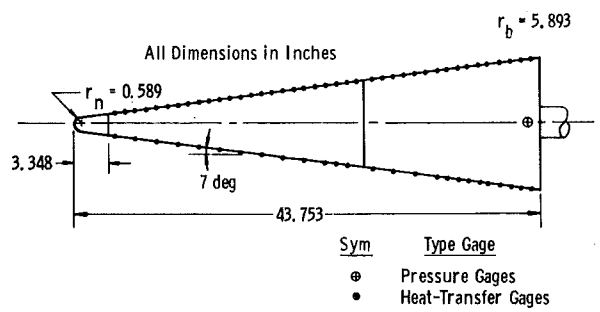

Fig. 2. Large Pressure-Heat-Transfer Model (7-deg Cone)

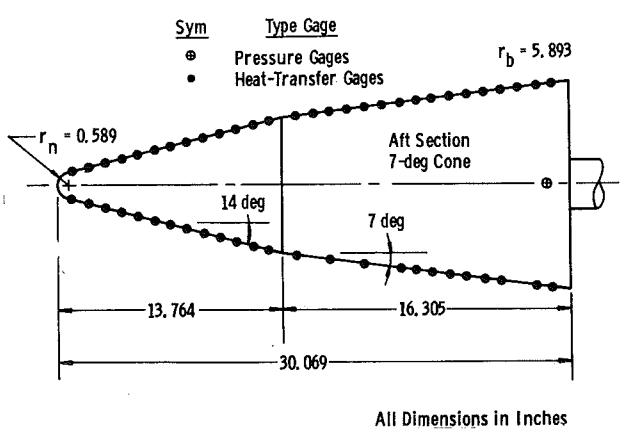

Fig. 3. The 14 → 7-deg Biconic Model

Table 1. Trip Descriptions

Type of Trip	Description
Grit Blast	Surface roughness was produced by impacting hardened steel particles onto the stainless-steel nose. RMS peak-to-valley roughness height was 5 mils. Roughness extended from s/r_n = 0 to 5. Roughness was determined by photomicrographs of samples.
Numerically Controlled Machine (NCM)	Roughness elements were machined as pyramids with a total height (peak-to-valley) of 8 and 14 mils. The base plane of the pyramids was recessed one-third of the height below the original unaltered model surface. The roughness extended from s/r_n = 0.1 to 5. Roughness was measured on optical comparators.
Grit	Roughness elements consisted of silicon carbide grit particles bonded to the model surface with epoxy. Grit sizes of 10, 14, 20, 36, and 40 mils were used, and coverage extended from s/r_n = 0.8 to 5. Roughness was defined by using Fig. A-3, Appendix A.
0.063- and 0.109-in. Spheres (7-deg Model)	Tripping elements consisted of two rows of spheres: a row of 0.063-in. spheres at s/r_n = 3.1 and a row of 0.109-in. spheres at s/r_n = 6.5. Lateral spacing was four diameters. The spheres were spot welded to thin metal bands that were then bonded to the model.
0.039-in. Spheres (14- and 7-deg Biconic)	Tripping elements consisted of a single row of 0.039-in. spheres at s/r_n = 6.8. The spheres were laterally spaced four diameters apart and spot welded to thin metal bands that were then bonded to the model surface.

3.0 Procedures

3.1 Test Conditions

Test conditions for the 40-in. nozzle of Tunnel F were as follows:

M_∞	Re_∞/ft x 10^{-6}	p_∞, psia	T_∞, °R	q_∞, psia
9.0	20.0	0.46	102	25.5
↓	18.0	0.43	107	24.5
↓	14.0	0.38	117	21.0
8.5	10.0	0.28	111	13.9
↓	8.0	0.25	123	13.0
↓	5.0	0.20	143	10.0
8.7	3.0	0.12	152	6.9
8.0	2.0	0.09	166	5.2

Conditions vary from run to run in Tunnel F, and the values listed above are nominal values.

3.2 Test Procedures

The latest tests complement previous work[1] in AEDC-VKF Tunnels B and F. The primary variables of Reynolds number, cone angle, and trip height were expanded in the current tests to promote a broad data base for correlation. Reynolds number was varied from 0.5 x 10^6 to 20.5 x 10^6 per foot, cone angle from 5 to 14 deg, and trip height from 5 to 40 mils. Angle of attack was maintained at zero, and model wall temperature ratio (T_w/T_{o_∞}) remained relatively constant at 0.15 to 0.35. A listing of primary variables is included in Appendix B along with a complete tabulation of the current test results.

4.0 Data Precision

For the Tunnel F tests, the uncertainties in measured data account for dynamics of the measurements and system errors. Representative values are given below.

Uncertainty (±), percent

M_∞	p_∞	T_∞	Re_∞/ft
3	7	8	11

5.0 Correlation of Results

In recent years, a great deal of interest has been generated in the area of roughness-induced transition on reentry vehicles. The commonly termed "PANT Correlation" has become an accepted standard in the design of reentry nosetips where roughness is present. Anderson[4] has shown that by using $Re_{e,\theta}$ as an amplification parameter and the expression $(T_e/T_w)(k/\theta)$ as a modified relative roughness, the PANT correlation is derived that can predict the onset and location of transition on a roughened nosetip. The equation thus arrived at is

$$\lambda = Re_{e,\theta}\left(\frac{T_e}{T_w}\,\frac{k}{\theta}\right)^{0.7} \quad \begin{array}{l}255\text{: required at}\\ =\text{ sonic point for}\\ \text{transition}\end{array} \qquad (1)$$

A. W. Mayne, ARO, Inc., has formulated a Reynolds-number-independent parameter, X, which makes the boundary-layer solutions necessary to apply the correlation a function of only M_∞ and T_w/T_{o_∞}. Laminar boundary-layer solutions, neglecting entropy swallowing (a reasonable assumption for hemispheres), were performed for flow over hemispheres with $2.5 \le M_\infty \le 20$ and constant wall temperatures in the range $0.05 \le T_w/T_{o_\infty} \le 1.0$. The gas was treated as thermally and calorically perfect air, with $T_\infty = 200^\circ R$ for $M_\infty = 2.5 \to 4$ and $T_\infty = 100^\circ R$ for $M_\infty > 4$. The boundary-layer solutions were performed using the methods described in Ref. 5. The parameter X was computed at the sonic point for each case.

Mayne assumed for a hemisphere that $T_e = C_1 T_{o_\infty}$, and using the similarity relationships

$$\frac{\theta}{r_n} \approx \frac{C_2}{\sqrt{Re_{\infty,r_n}}} \quad \text{and} \quad Re_{e,r_n} = C_3\, Re_{\infty,r_n}$$

(where C_1, C_2, and C_3 are constants), the PANT formula became

$$\lambda^* = X\left(\frac{k}{r_n}\right)^{0.7}\left(Re_{\infty,r_n}\right)^{0.85} \quad \begin{array}{l}255\text{ for effective}\\ =\text{ tripping on}\\ \text{the nosetip}\end{array} \qquad (2)$$

where

$$X = Re^*_{e,\theta}\left[\frac{T^*_e}{T_w}\,\frac{r_n}{\theta^*}\right]^{0.7}\frac{1}{\left(Re_{\infty,r_n}\right)^{0.85}} \qquad (3)$$

The * superscript indicates conditions evaluated at the sonic point. Figure A-1 (Appendix A) presents X as a function of T_w/T_{o_∞} with M_∞ as a parameter.

It should be noted that the PANT correlation and Mayne's reformulation of it are meant to predict transition on the hemispherical section of a nosetip only. It does not account for any "laminarization" that might occur as a result of the expansion around the shoulder. When one attempts to use λ^* as a correlating parameter for distributed roughness on blunt-slender cones (see Fig. 4), the results are not satisfactory. One notes, for instance, a strong dependence on Mach number for which λ^* fails to account. This most likely is caused by the expansion process that, of course, is a strong function of M_∞ and cone angle. If a $\lambda^*_{critical}$ is defined as that λ^* required to bring the end of transition, s_t, up to a point near the trip, from Fig. 4 one can cross-plot $\lambda^*_{critical}$ versus M_∞ as shown in Fig. 5a. A definite correlation with Mach number is noted. Cone angle also has an effect on $\lambda^*_{critical}$ as noted in Fig. 5b. The Mach number and cone angle dependence of λ^* clearly points to a requirement of adding (to the PANT correlation) a term that characterizes the expansion process when the correlation is to be applied to the conical section of a body. This term must account for variations in the strength of the expansion attributable to changes in Mach number and cone angle.

Analysis indicated that the ratio of local static pressure at the end of the gritted area (P_E) to the pitot pressure, P'_o, would effectively characterize the expansion. Hence, P_E/P'_o alone accounts for both Mach number and cone angle variations.

Hence, a modified λ^* may be defined as

$$\lambda^*_M = (X) f\left(\frac{k}{r_n},\ Re_{\infty,r_n},\ \frac{P_E}{P'_o}\right) \qquad (4)$$

One would expect, of course, that the relationships among the various terms of Eq. (4) would differ from the PANT formulation since the equation is being applied to a physically and aerodynamically different part of the body. The PANT formulation and Mayne's reformulation are valuable, however, in that they identify the significant variables.

Sym	θ_c, deg	r_n, in.	k, mils	M_∞	Source
♦	8.0	2.50	1.6	5.0	PANT, AFML-TR-74-147
•	8.0	2.45	10.0	7.9	PANT, NOLTR-73-231
•	6.3	0.125	5.0	8.8	Tunnel F Data
•	7.0	0.589	5.0	10.5	Tunnel F Data
✱	7.0	0.589	14.0	13.0	Tunnel F Data
▪	7.0	0.589	14.0	8.0	Tunnel B Data

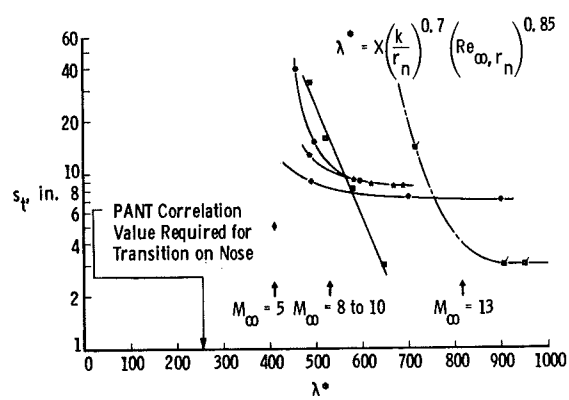

Fig. 4. Correlation of Distributed-Roughness Tripping Results with the PANT Parameter λ^*

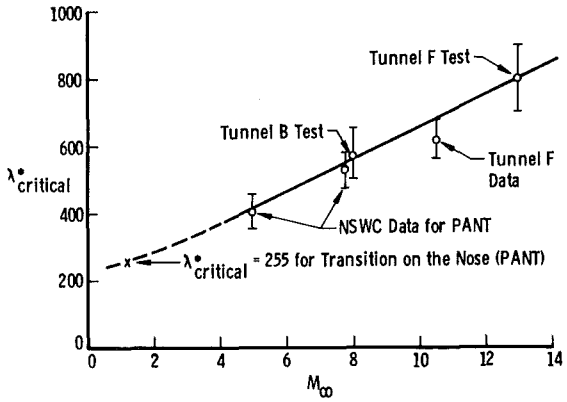

a. Mach Number Effects on $\lambda^*_{critical}$

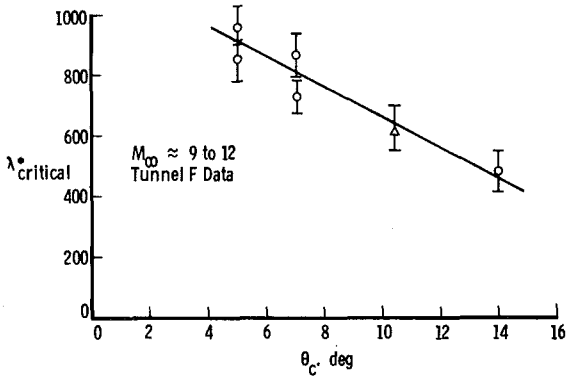

b. Variation of $\lambda^*_{critical}$ with Cone Angle

Fig. 5. Effects of Mach Number and Cone Angle on $\lambda^*_{critical}$

Applying an analysis of these variables to the previous data[1] and the present results, a correlation was derived as shown in Fig. 6. As one may note from the limits listed in the figure, a fairly wide range of variables has been correlated. Special note should be taken of the limits on k/r_n. Obviously one could choose a combination of variables outside these limits (i.e., low Re_∞/ft, r_n, and θ_c) that would yield unrealistic values of k/r_n. Within the stated limits, however, the correlation appears quite good.

The combination of cold-wall models and hypersonic wind tunnels operating at saturation temperatures yielded an essentially constant value of X (X ≈ 0.3). Hence, the new correlation becomes

$$\lambda^*_M = X\left(\frac{k}{r_n}\right)\left(\frac{P_E}{P'_o}\right)^{0.9}\left(Re_{\infty,r_n}\right)^{1.2} \qquad (5)$$

and

$$\lambda^*_{M_{critical}} \approx 800 \qquad (6)$$

for transition immediately behind the trip location. Therefore, for effective tripping with distributed-roughness-type trips, $\lambda^*_M \geq 800$. One should note that the roughened area should extend approximately from 45 deg off the stagnation point to $s/r_n = 5$, as pointed out in the previous work.[1] The $s/r_n = 5$ criterion for the termination of roughness appears to be adequate in terms of overcoming the expansion process and at the same time practical in terms of the amount of area roughened. Its use is highly recommended by the author.

Sym	Source
○	Current Results at $M_\infty = 9$
□	Tunnel B Results, Ref. 1
△	Tunnel F Results, Ref. 1
☆	FY 78 Results, Tunnel B, $M_\infty = 6$
◇	AEDC-VKF Data, Tunnel B, $M_\infty = 6$
▽	AEDC-VKF Data, Tunnel F, $M_\infty = 12.7$
▯	PANT Data, NOL-TR-73-231

NOTE: The majority of data used in this correlation is based upon roughness extending to $s/r_n \approx 5$.

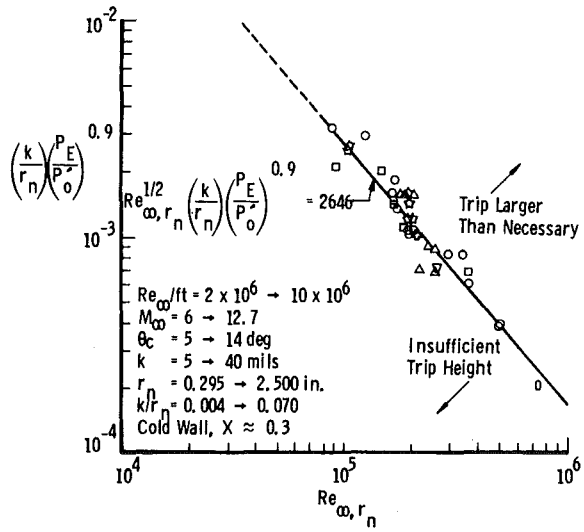

Fig. 6. Distributed-Roughness Tripping Correlation

One may solve Eq. (5) for k by obtaining an appropriate value of X from Fig. A-1 of Appendix A and likewise a value of P_E/P'_o from Fig. A-2 (where P_E/P'_o is evaluated at $s/r_n = 5$). Values of k are correlated with standard grit number in Fig. A-3.

It has been widely observed that trip effectiveness is somewhat related to the natural (untripped) transition location. The natural transition location in turn is a function of the nose radius as observed by Stetson and Rushton.[6] Therefore, one would want a correlation for tripping to be applicable at the worst condition, i.e., the nose radius that produces the greatest rearward displacement of natural transition location. Figure 7 shows that this is indeed the case for the correlation presented herein. Data[7] from the 7-deg cone (Fig. 1) indicate that the maximum rearward displacement of the beginning of transition occurs between r_n = 0.259 and 0.884 in., which is the range of most data used in Fig. 6. It should be noted that the majority of data correlated in Fig. 6 are for r_n = 0.500 → 0.589 in.; only four data points fall outside that range.

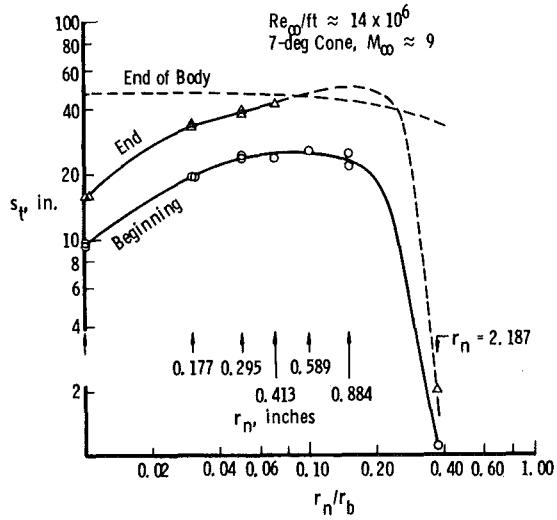

Fig. 7. Blunt Cone Natural Transition at Re_∞/ft ≈ 14 x 10^6

6.0 Conclusions

1. The unmodified PANT formula fails to correlate roughness-induced transition on the conical sections of blunt slender cones.

2. Both Mach number and cone angle effects must be accounted for in an adequate correlation parameter.

3. The inviscid pressure ratio P_E/P_o' at $s/r_n = 5$ adequately models the expansion process (hence the Mach number and cone angle effects) on blunt cones.

4. Blunt cone roughness-induced transition data can be correlated using a modified version of the PANT correlation:

$$\lambda_M^* = X\left(\frac{k}{r_n}\right)\left(\frac{P_E}{P_o'}\right)^{0.9}\left(Re_{\infty,r_n}\right)^{1.2}$$

where

$$\lambda^*_{M_{critical}} = 800$$

5. Roughness should extend from $s/r_n = 0.8$ to 5 for adequate tripping.

6. The present correlation represents the range of nose radii that are most difficult to trip.

References

[1]Boudreau, A. H., "Artificially Induced Boundary-Layer Transition on Blunt-Slender-Cones Using Distributed Roughness and Spherical Type Tripping Devices at Hypersonic Speeds," AIAA Paper 78-1127, presented at the AIAA 11th Fluid and Plasma Dynamics Conference, Seattle, Washington, July 10-12, 1978.

[2]Test Facilities Handbook (Tenth Edition), "von Kármán Gas Dynamics Facility, Vol. 3," Arnold Engineering Development Center, May 1974.

[3]Pate, S. R. and Eaves, R. H., Jr., "Recent Advances in the Performance and Testing Capabilities of the AEDC-VKF Tunnel F (Hotshot) Hypersonic Facility," AIAA Paper No. 74-84, presented at the AIAA 12th Aerospace Sciences Meeting, Washington, D. C., January 30 - February 1, 1974.

[4]Anderson, Aemer D. "Boundary-Layer Transition on Nosetips with Rough Surfaces." Appendix to Vol. X of "Interim Report Passive Nosetip Technology (PANT) Program," SAMSO-TR-74-86 (AD-A020708), Vols. I-XV, January 1975.

[5]Mayne, A. W., Jr. and Dyer, D. F., "Comparison of Theory and Experiment for Turbulent Boundary Layers on Simple Shapes at Hypersonic Conditions," Proceedings of the 1970 Heat-Transfer and Fluid Mechanics Institute, Stanford University Press, 1970, pp. 168-188.

[6]Stetson, Kenneth F. and Rushton, George H., "Shock Tunnel Investigation of Boundary-Layer Transition at M = 5.5, AIAA Journal, Vol. 5, May 1967.

[7]Stetson, Kenneth F., "Effect of Bluntness and Angle-of-Attack on Boundary-Layer Transition on Cones and Biconic Configurations," AIAA Paper 79-0269, presented at the AIAA 17th Aerospace Sciences Meeting, New Orleans, LA, January 15-17, 1979.

Appendix A
Plots for Use with the λ^* Correlation

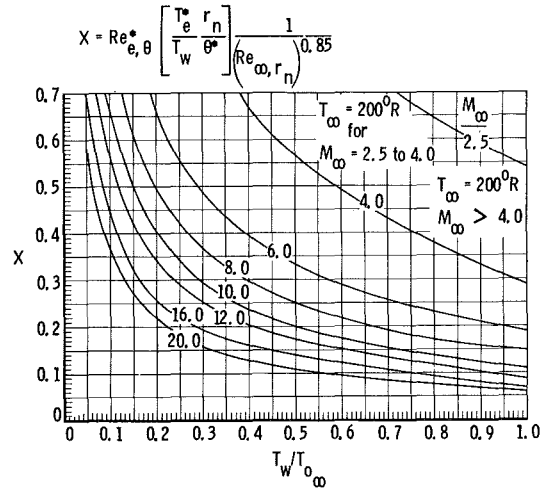

Fig. A-1. Correlation Similarity Parameter for Thermally and Calorically Perfect Air

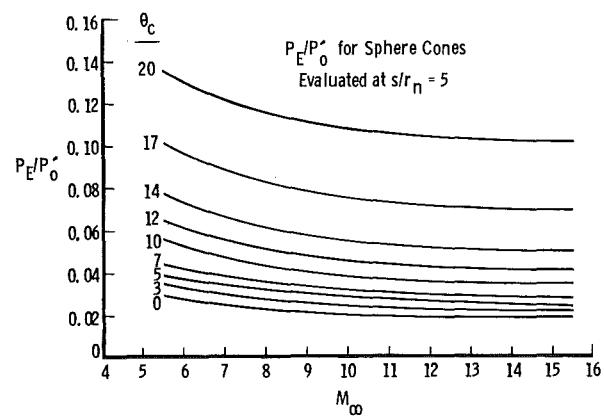

Fig. A-2. Inviscid 3-D Characteristics Pressure Ratio for $s/r_n = 5$

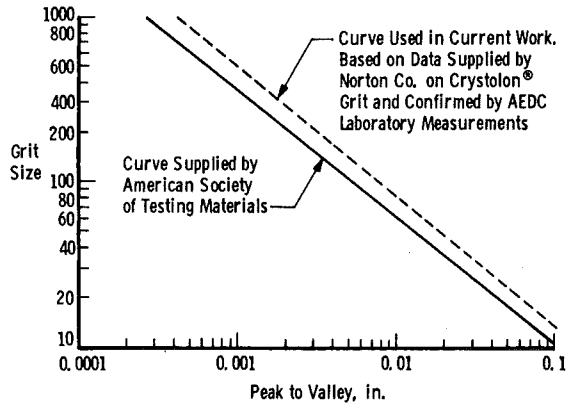

Fig. A-3. Correlation of Grit Number with Nominal Peak-to-Valley Distance

Appendix B
Tabulated Results

Model	Data Group	M_∞	Re_∞/ft x 10^{-6}	$r_{n'}$ in.	k, in.	Type Trip[2]	Extent of s/r_n Range	$s_{t'}$[1] in.
5-deg	6020	8.3	10.1	0.5	0.014	Distributed Grit	0.8 - 5.0	5
		8.3	8.2					5
		8.5	5.0					5
		8.5	4.0					7
		8.6	3.0					10
		8.7	2.5					22
		8.7	2.0					30
5-deg	6021	8.2	10.0	0.5	0.020	Distributed Grit	0.8 - 5.0	5
		8.3	8.1					5
		8.4	5.0					5
		8.5	4.1					5
		8.9	3.0					10
		9.2	2.5					28
		9.3	2.0					Transition
		9.4	1.5					Laminar
5-deg	6022	8.1	10.5	0.5	0.036	Distributed Grit	0.8 - 5.0	5
		8.2	8.2					5
		8.3	5.3					5
		8.4	4.1					5
		8.6	3.0					5
		9.0	2.5					30
		9.2	2.0					Transition
		9.2	1.7					
5-deg	6023	8.9	18.2	0.5	0.010	Distributed Grit	0.8 - 5.0	5
		8.8	14.3					5
		8.6	10.2					5
		8.4	8.2					8
		8.2	6.0					25
		8.1	5.1					Transition
5-deg	6024	8.1	10.3	0.5	0.010	Distributed Grit	0.8 - 5.0	5
		8.4	7.1					5
		8.5	5.2					7
		8.6	4.1					10
		8.7	3.5					28
		8.9	3.0					Transition
		9.0	2.5					Laminar
		9.0	2.3					Laminar
7-deg	6005	9.0	20.3	0.589	No	Trips	---	33
		9.1	17.9					41
		9.0	13.9					44
		8.8	10.1					Transition
		8.7	8.1					
		8.6	6.3					
7-deg	6006	8.9	20.5	0.589	0.005	Grit Blasted	0.0 - 5.0	4
		9.1	18.1					4
		9.0	14.0					4
		8.8	10.0					4
		8.8	8.0					44
		8.7	6.0					Transition
7-deg	6007	8.4	5.1	0.589	0.014	Distributed Grit	0.8 - 5.0	4
		8.3	4.0					4
		8.3	3.1					6
		8.4	2.5					30
		8.3	2.0					31
		8.5	1.8					Transition
7-deg	6008	8.7	4.5	0.589	0.014	NCM	0.10 - 5.0	4
		8.8	4.0					4
		9.0	3.5					31
		8.8	2.5					40
		8.7	2.0					Transition
		8.7	1.7					Laminar
7-deg	6009	8.0	3.1	0.589	0.040	Distributed Grit	0.8 - 5.0	4
		8.0	2.6					4
		8.3	2.0					4
		8.3	1.6					6
		8.4	1.0					31
		8.6	0.8					Transition
		8.5	0.5					Laminar
7-deg	6010	8.2	10.3	0.589	0.005	Distributed Grit	0.0 - 5.0	4
		8.7	8.2					5
		8.2	5.2					8
		8.1	4.0					14
		8.1	3.0					44
		8.3	2.6					Transition
		8.5	2.0					Laminar
		8.6	1.5					
		8.8	1.1					
7-deg	6011	8.4	5.9	0.589	0.063 & 0.109	Spheres	3.1 & 6.5	4
		8.6	4.0					4
		8.9	3.7					30
		9.0	3.6					31
		9.3	4.0					31
		9.3	3.7					32
		9.3	3.0					32
		9.2	2.5					34
		8.8	1.9					Transition
7-deg	6012	8.5	8.0	0.589	0.063 & 0.109	Spheres	3.1 & 6.5	4
		8.2	5.1					4
		8.3	4.0					4
		8.7	3.0					30
		9.1	2.0					32
7-deg	6013	8.5	10.0	0.589	0.008	NCM	0.10 - 5.0	4
		8.7	7.5					6
		8.4	5.1					29
		8.5	4.0					33
		8.8	3.5					35
		9.1	3.0					44
		8.6	2.5					Transition
Biconic	6016	8.9	20.8	0.589	No	Trips	---	30
		8.9	18.6					30
		9.1	14.3					30
		8.8	10.2					30
		8.6	8.1					Transition
		8.6	7.6					Transition
Biconic	6017	8.2	5.2	0.589	0.014	Distributed Grit	0.8 - 5.0	3
		8.4	4.0					3
		8.6	3.5					3
		8.8	3.0					14
		8.6	2.8					Transition
		8.7	2.5					
		8.4	2.0					
Biconic	6018	8.3	5.1	0.589	0.039	Spherical	6.8	5
		8.4	4.0					8
		9.1	3.1					14
		9.3	2.5					14
		9.4	2.0					14
		9.3	1.7					Transition
Biconic	6019	8.3	10.3	0.589	0.010	Distributed Grit	0.8 - 5.0	3
		8.4	7.5					3
		8.3	5.1					3
		8.3	4.0					3
		8.5	3.5					3
		9.0	3.1					14
		8.8	2.5					14
		8.6	2.3					14

[1] Minimum determinable s_t values are:

5-deg cone: 5 in.
7-deg cone: 4 in.
Biconic: 3 in.

[2] See Table 1.